Electronic Supplementary Information

Ratiometric fluorescence sensing and intracellular imaging of Al^{3+} ion driven by an intramolecular excimer formation of a pyrimidine-pyrene scaffold

Sudipta Das,[a] Animesh Sahana,[a] Arnab Banerjee,[a] Sisir Lohar,[a] Damir A. Safin,*[b] Maria G. Babashkina,[b] Michael Bolte,[c] Yann Garcia,[b] Ipsit Hauli,[d] Subhra Kanti Mukhopadhyay[d] and Debasis Das*[a]

[a] *Department of Chemistry, The University of Burdwan, Burdwan, 713104, West Bengal, India. Fax: +91 342 2530452; Tel: +91 342 2533913; E-mail: ddas100in@yahoo.com*

[b] *Institute of Condensed Matter and Nanosciences, MOST - Inorganic Chemistry, Université Catholique de Louvain, Place L. Pasteur 1, 1348 Louvain-la-Neuve, Belgium. Fax: +32(0) 1047 2330; Tel: +32(0) 1047 2831; E-mail: damir.safin@ksu.ru*

[c] *Institut für Anorganische Chemie J.-W.-Goethe-Universität, Frankfurt/Main, Germany*

[d] *Department of Microbiology, The University of Burdwan, Burdwan 713104, India*

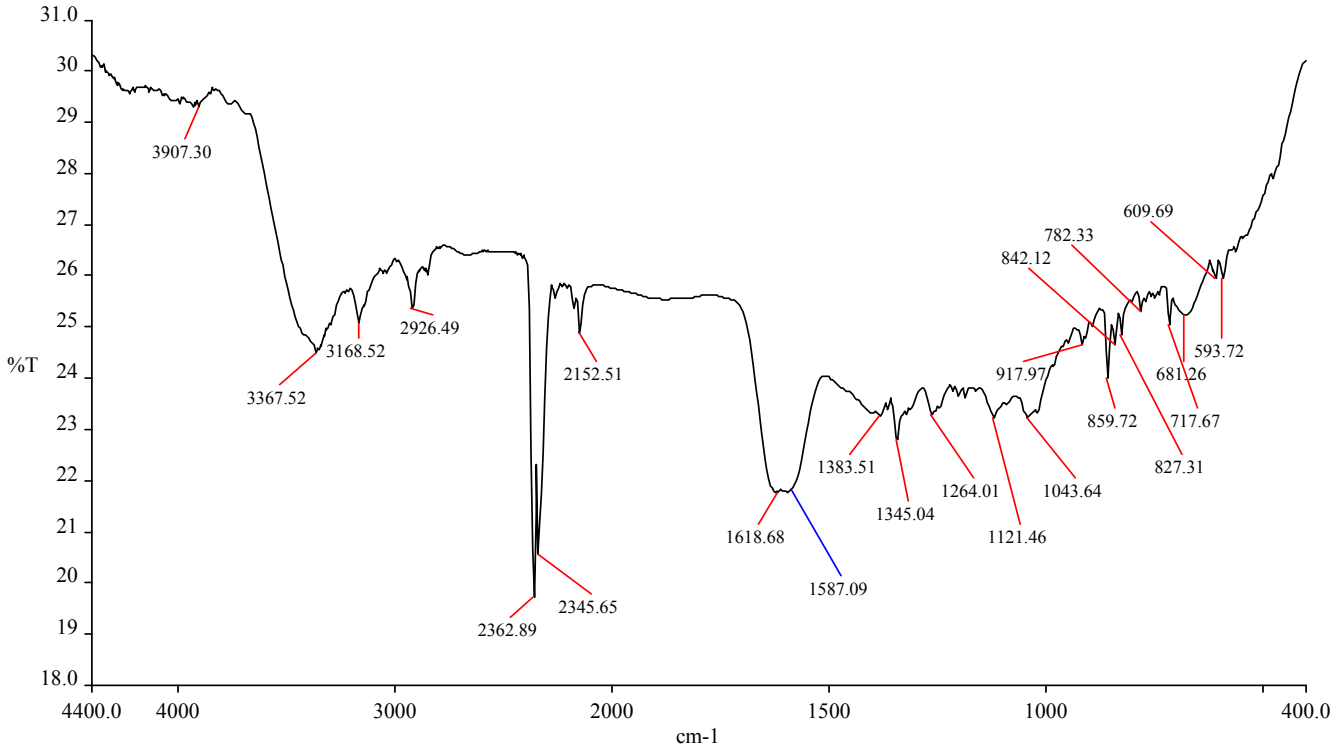

Fig. S1 FTIR spectrum of **L**.

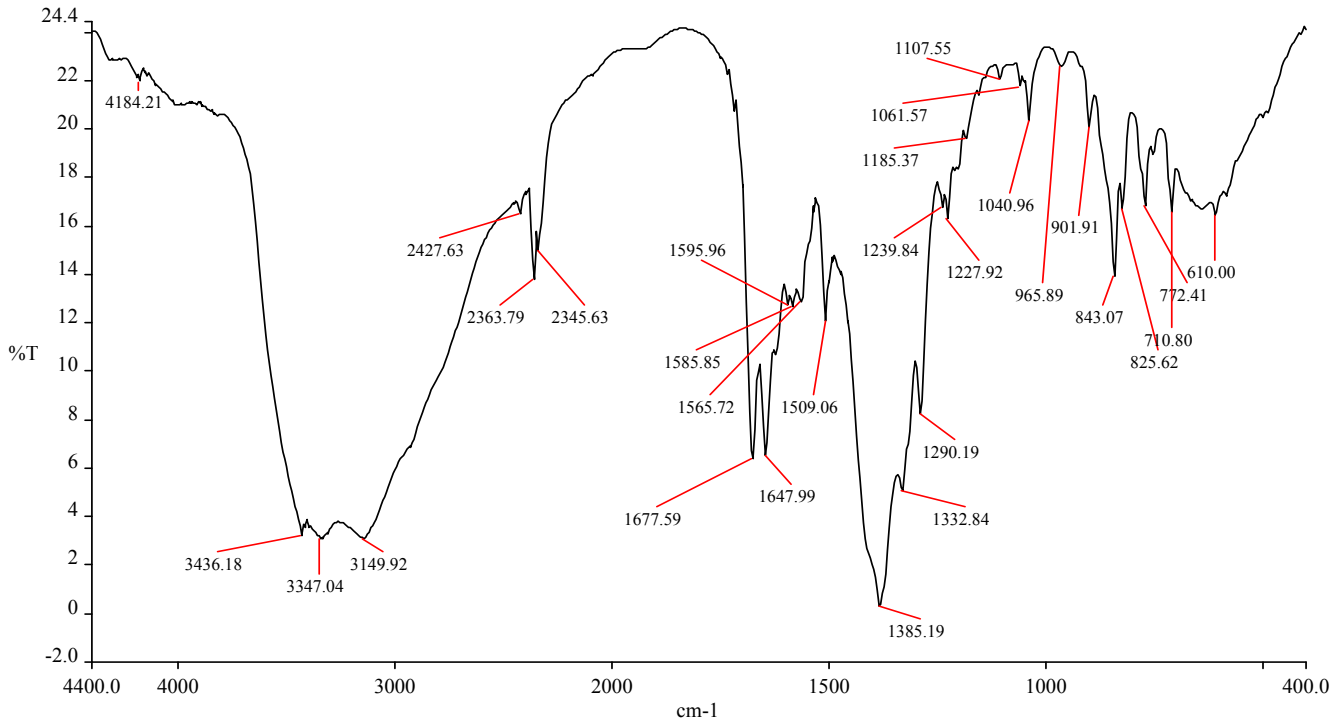

Fig. S2 FTIR spectrum of [**L**–Al^{3+}].

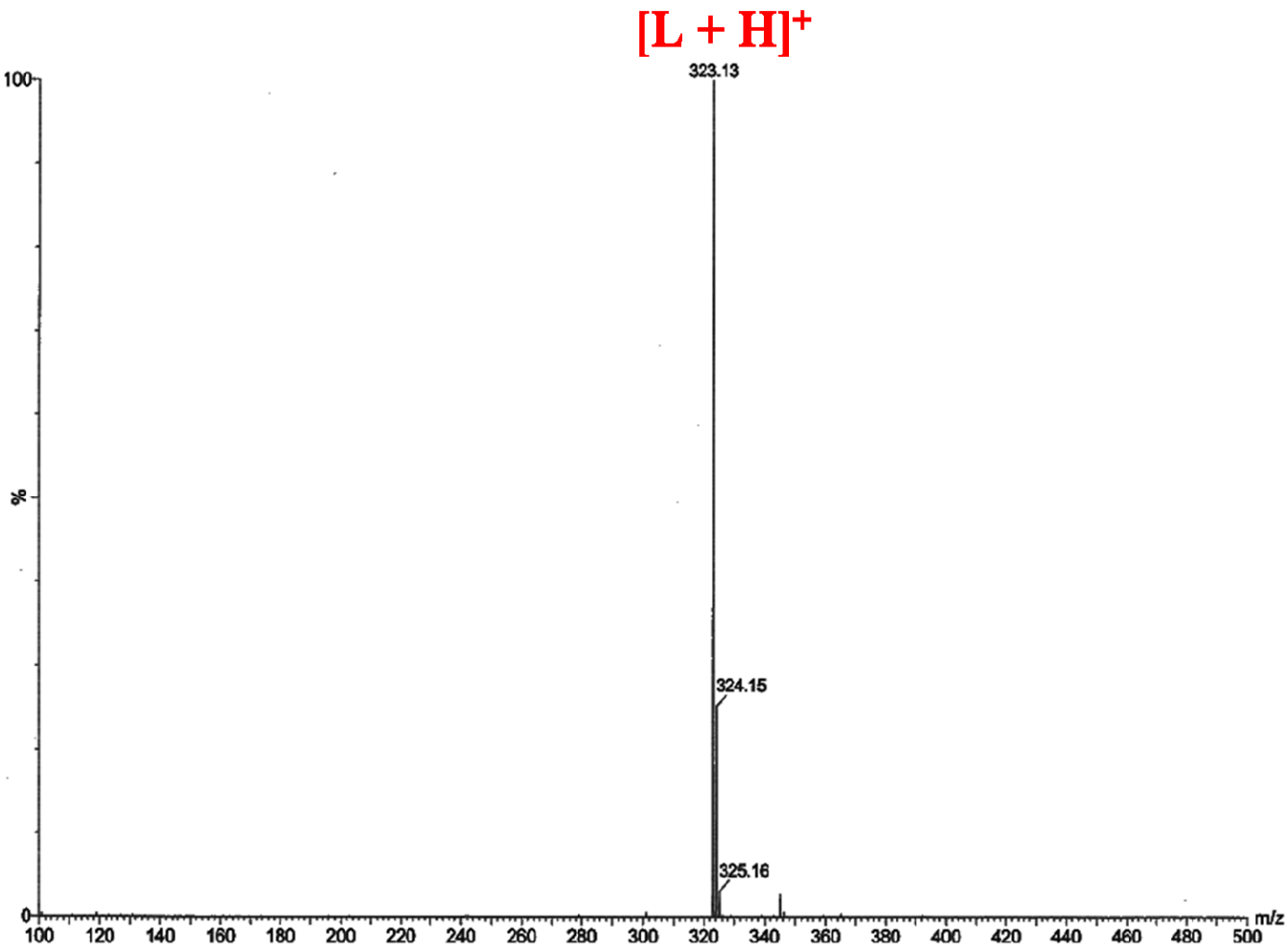

Fig. S3 ESI-MS$^+$ spectrum of **L**.

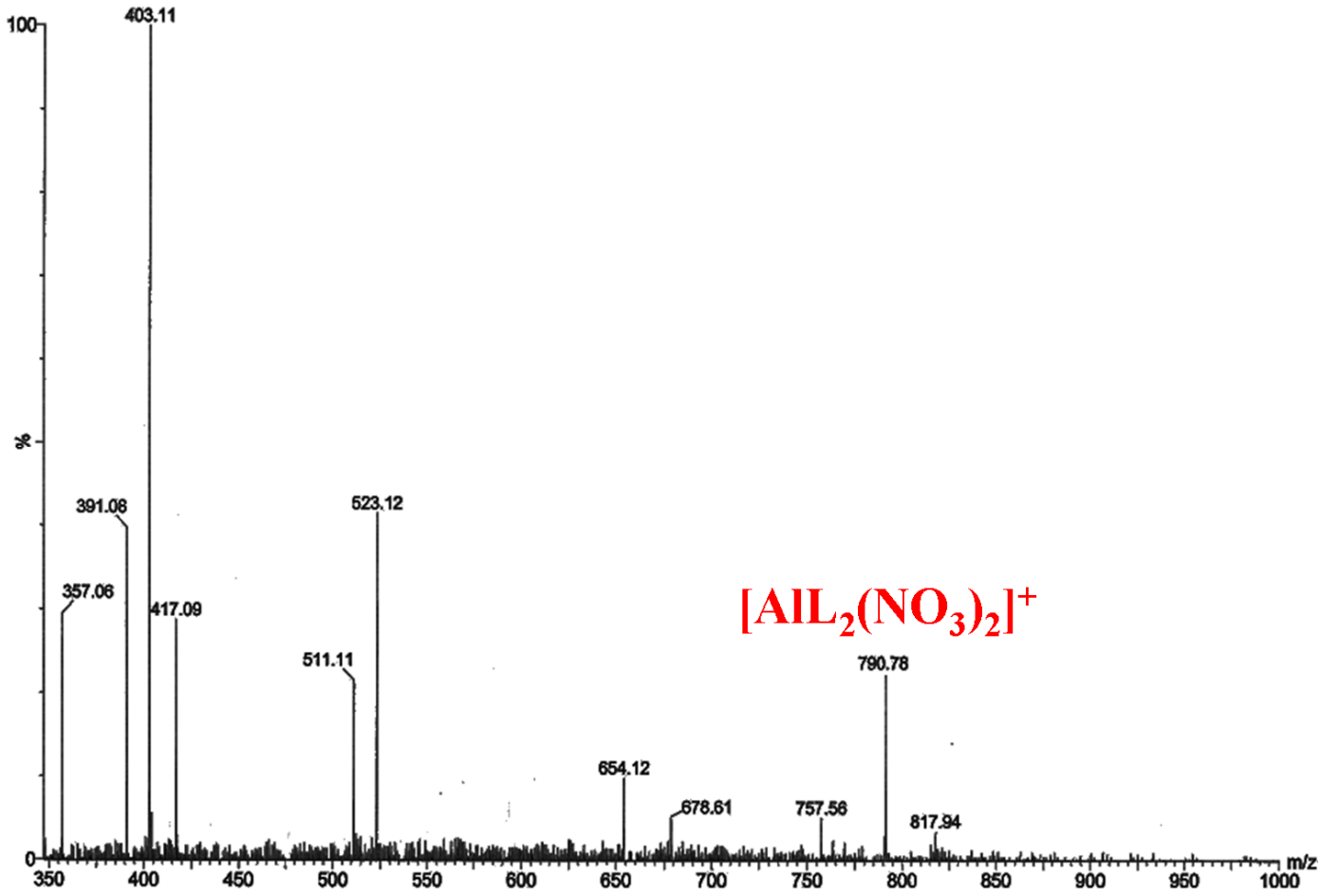

Fig. S4 ESI-MS$^+$ spectrum of $[Al\mathbf{L}_2(NO_3)_2]^+$.

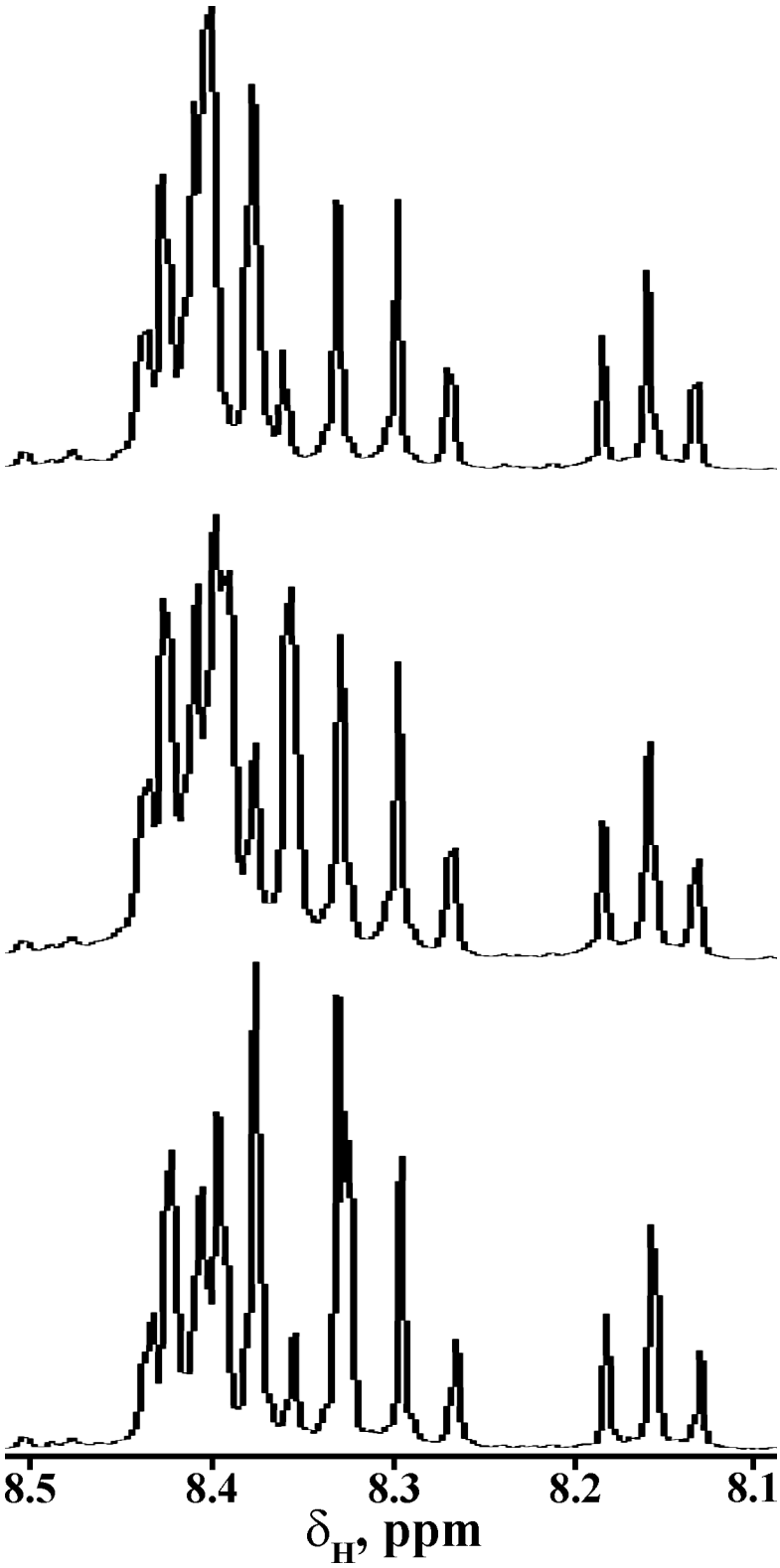

Fig. S5 Enlarged view of the 8.1–8.5 ppm range of the ^{1}H NMR spectra of **L** (bottom), **L** + 0.5 eqv. Al^{3+} (middle) and **L** + 1 eqv. Al^{3+} (top).

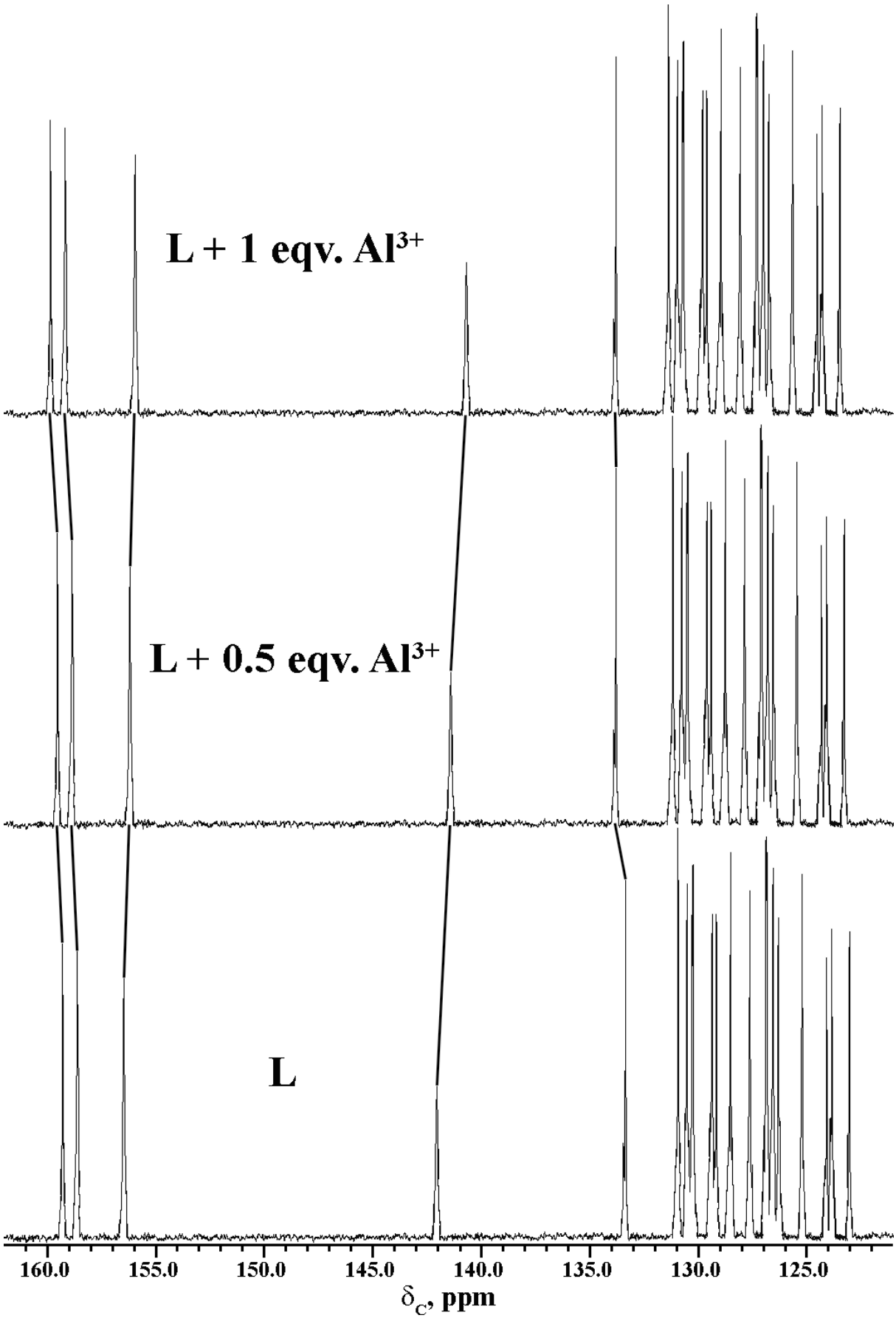

Fig. S6 ^{13}C NMR titration of **L** by $Al(NO_3)_3 \cdot 9H_2O$ in DMSO-d_6.

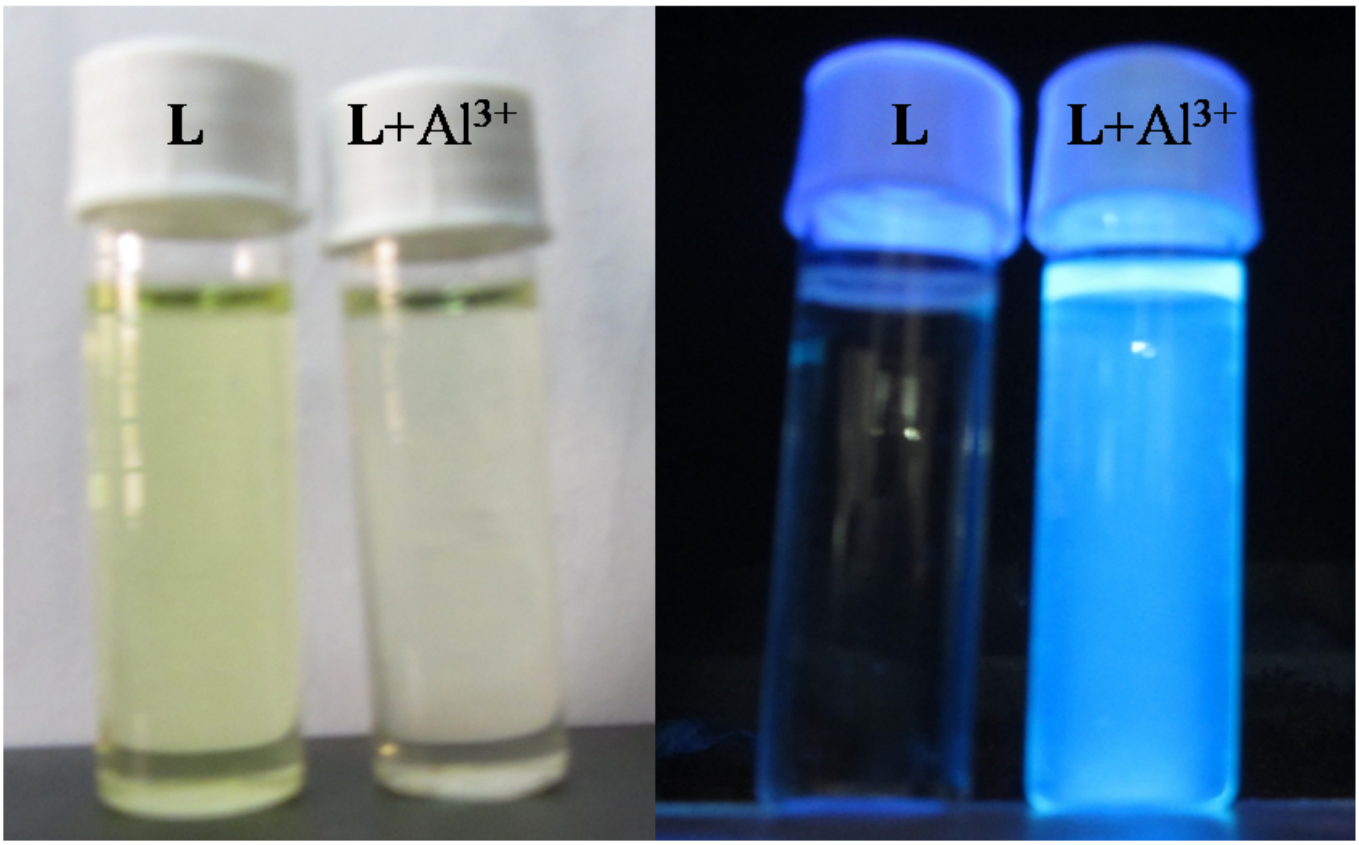

Fig. S7 Color change of a solution of **L** after addition of equivalent quantity of Al^{3+}: under ambient light (left) and under UV light (right).

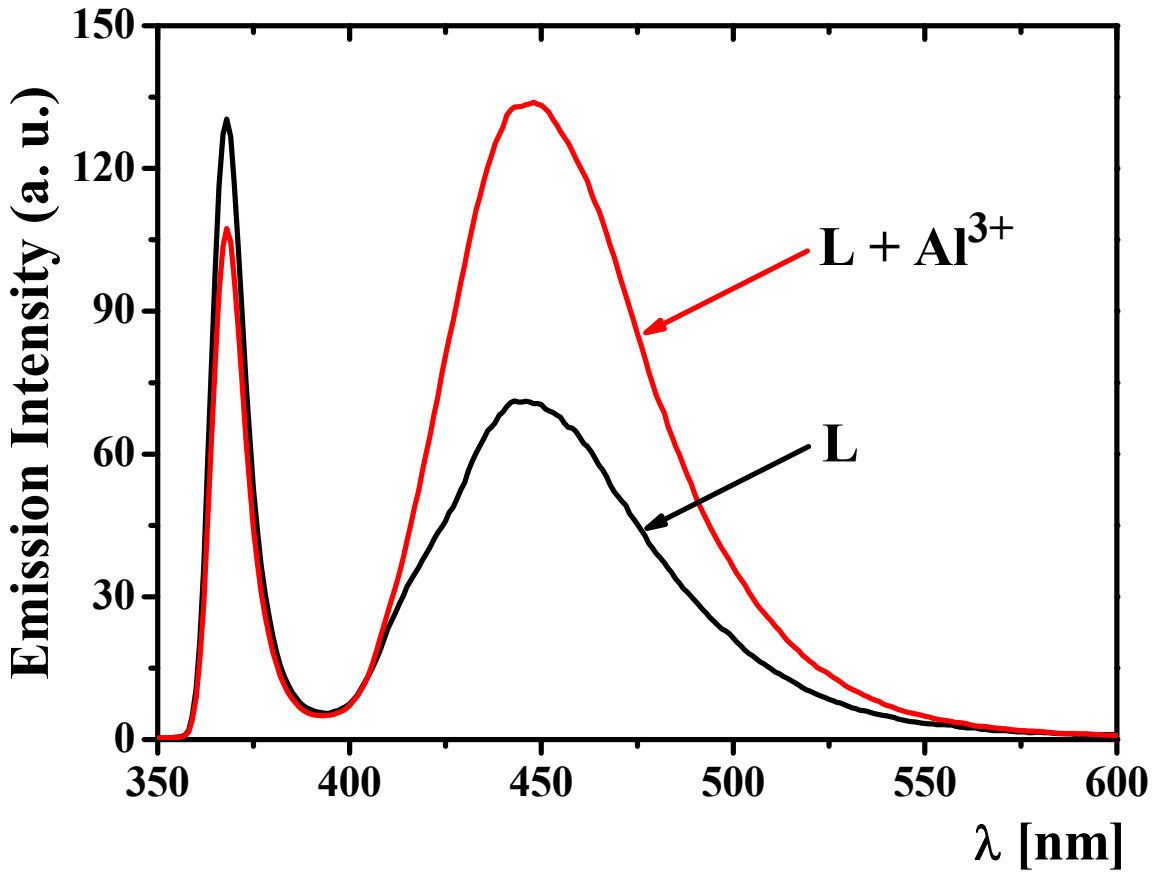

Fig. S8 Emission spectra of **L** and its Al^{3+} complex with λ_{ex} = 290 nm ([**L**] = 5 μM, [Al^{3+}] = 50 μM, DMSO–H_2O, 4:1, v/v, 0.1 M HEPES buffer, pH 7.4).

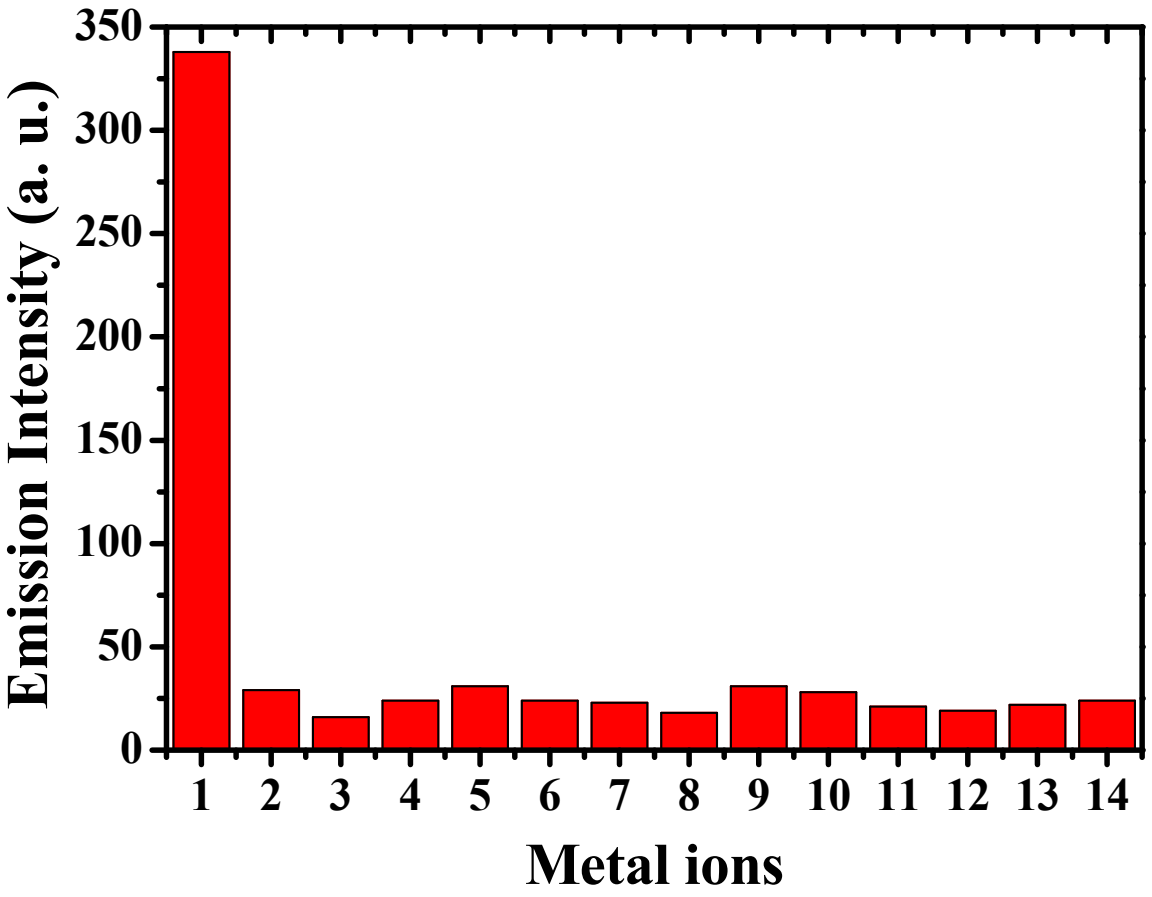

Fig. S9 Emission intensities of **L** (5 μM) + Al^{3+} (110 μM) (**1**) and **L** (5 μM) + M^{n+} (150 μM), where M^{n+}: (**2**) Na^{+}, (**3**) Mg^{2+}, (**4**) Cr^{3+}, (**5**) Mn^{2+}, (**6**) Fe^{3+}, (**7**) Co^{2+}, (**8**) Ni^{2+}, (**9**) Cu^{2+}, (**10**) Zn^{2+}, (**11**) Hg^{2+}, (**12**) Pb^{2+}, (**13**) Cd^{2+}, (**14**) Ag^{+} (as their nitrate salts) (DMSO–H_2O (4:1, v/v), 0.1 M HEPES buffer, pH 7.4, λ_{ex} = 330 nm, λ_{em} = 445 nm).

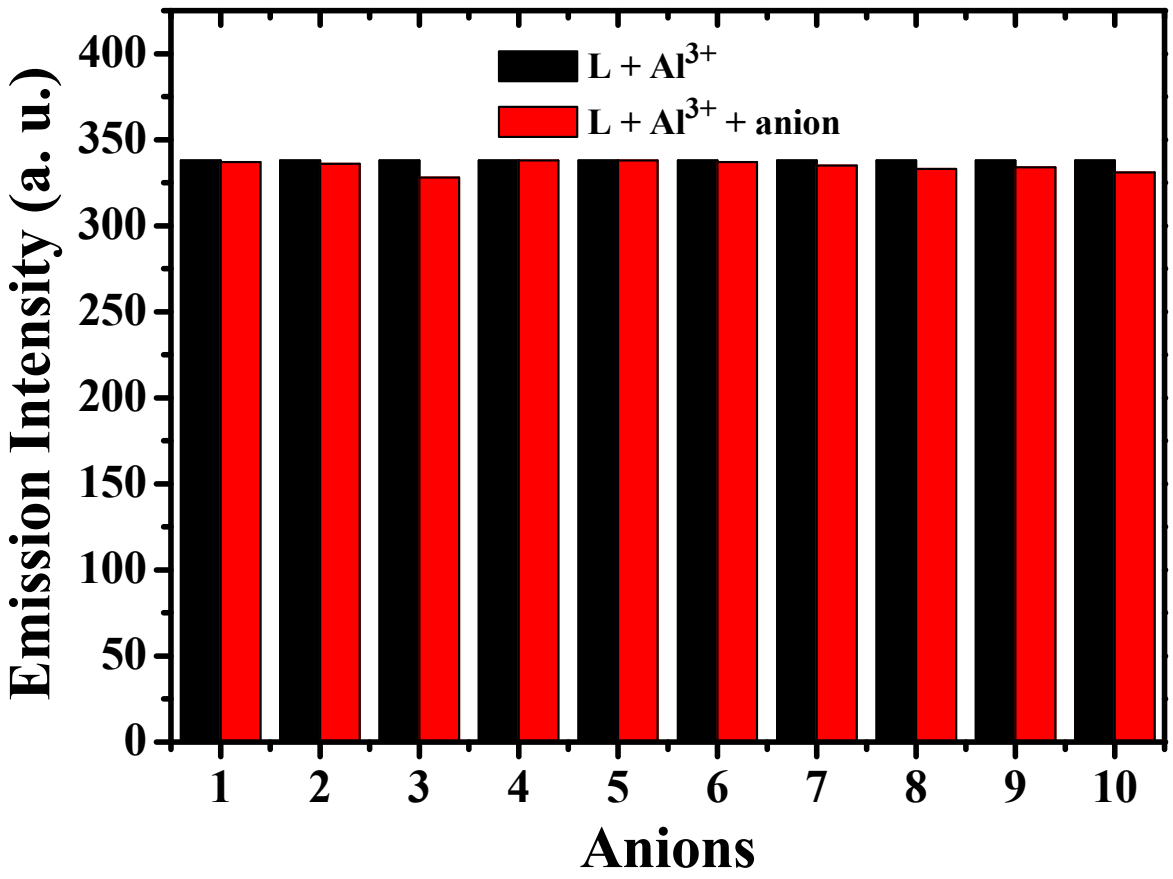

Fig. S10 Interference of different anions (as their sodium salts) [SO_4^{2-} (**1**), Cl^- (**2**), F^- (**3**), I^- (**4**), N_3^- (**5**), NO_2^- (**6**), NO_3^- (**7**), HSO_4^- (**8**), CH_3COO^- (**9**), $H_2PO_4^-$ (**10**)] on the determination of [Al^{3+}] by **L** (DMSO–H_2O (4:1, v/v), 0.1 M HEPES buffer, pH 7.4, λ_{ex} = 330 nm, λ_{em} = 445 nm). [**L**] = 5 μM, [Al^{3+}] = 110 μM and [anion] = 150 μM.

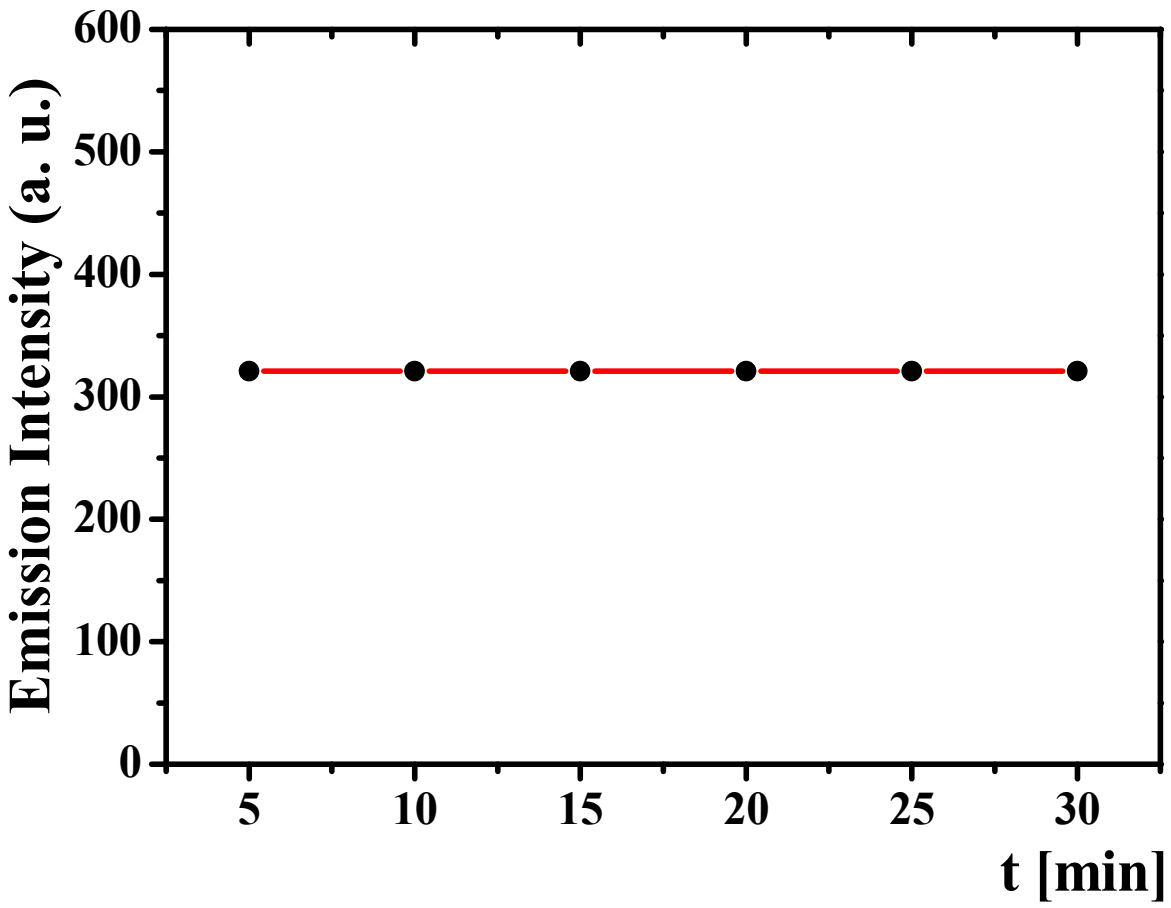

Fig. S11 Plot of variation of fluorescence intensity with time. [**L**] = 5 μM, [Al^{3+}] = 110 μM (DMSO–H_2O (4:1, v/v), 0.1 M HEPES buffer, pH 7.4, λ_{ex} = 330 nm, λ_{em} = 445 nm).

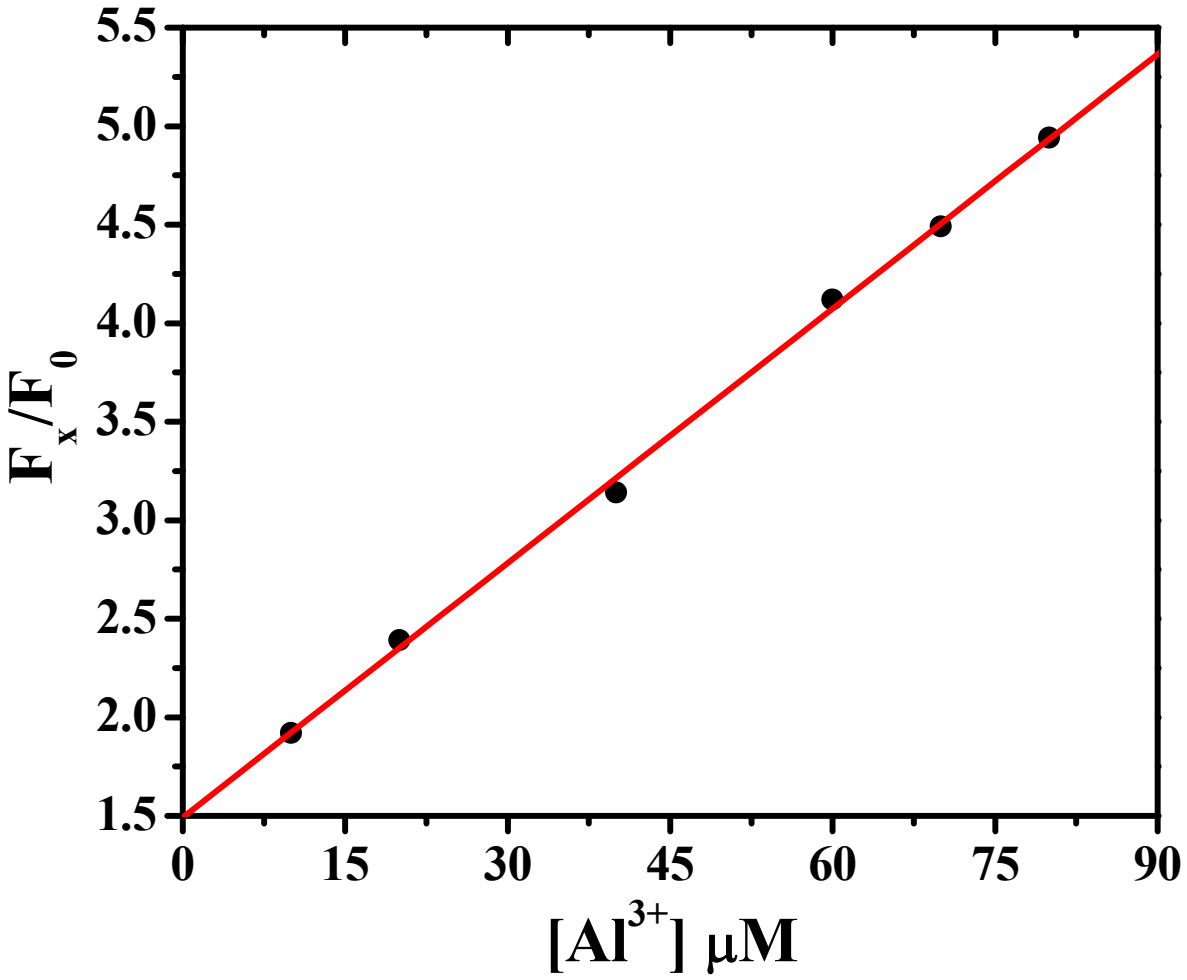

Fig. S12 Determination of the detection limit of Al^{3+} by **L** (5 μM) (DMSO–H_2O (4:1, v/v), 0.1 M HEPES buffer, pH 7.4, λ_{ex} = 330 nm, λ_{em} = 445 nm) (R^2 = 0.99).

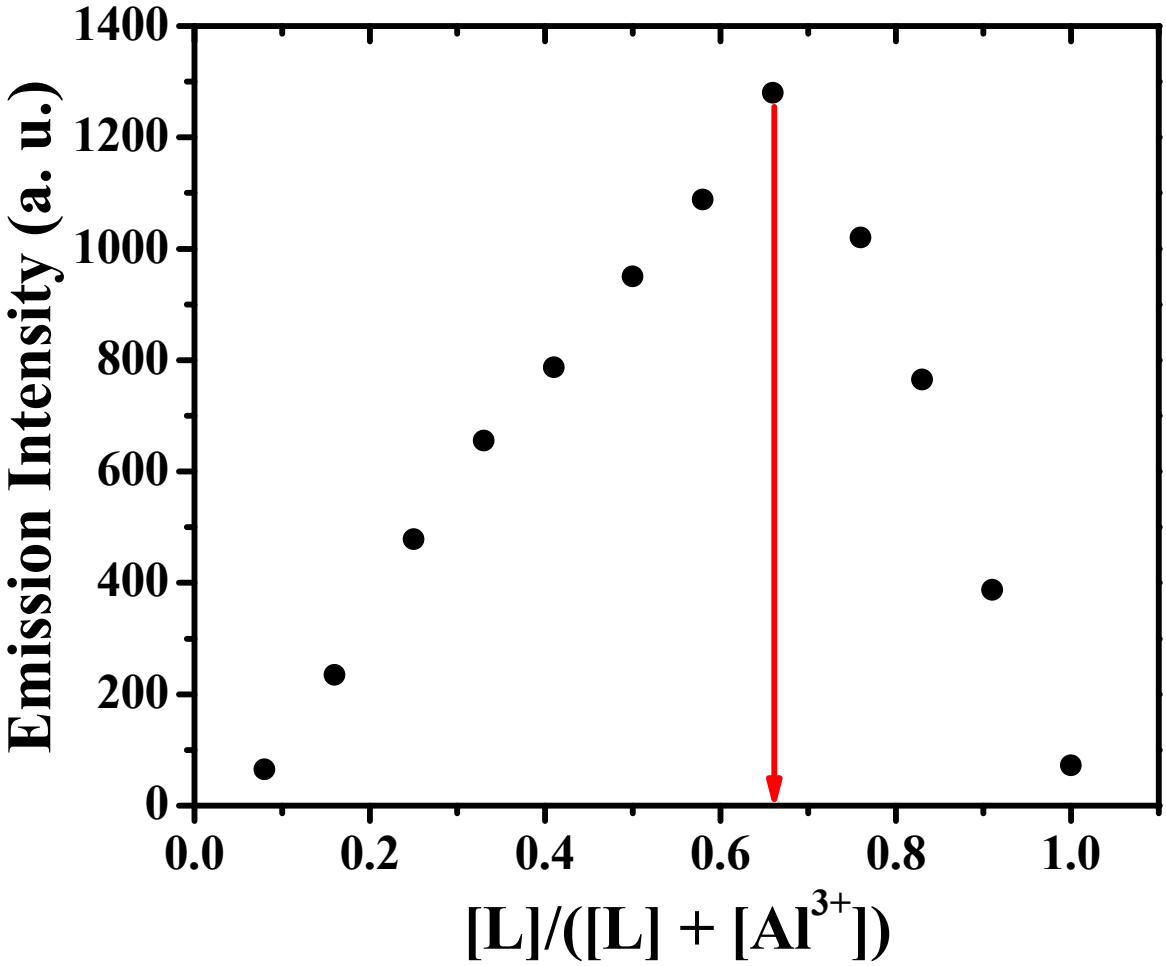

Fig. S13 Job's plot for the determination of a stoichiometry of the [**L**–Al^{3+}] system.

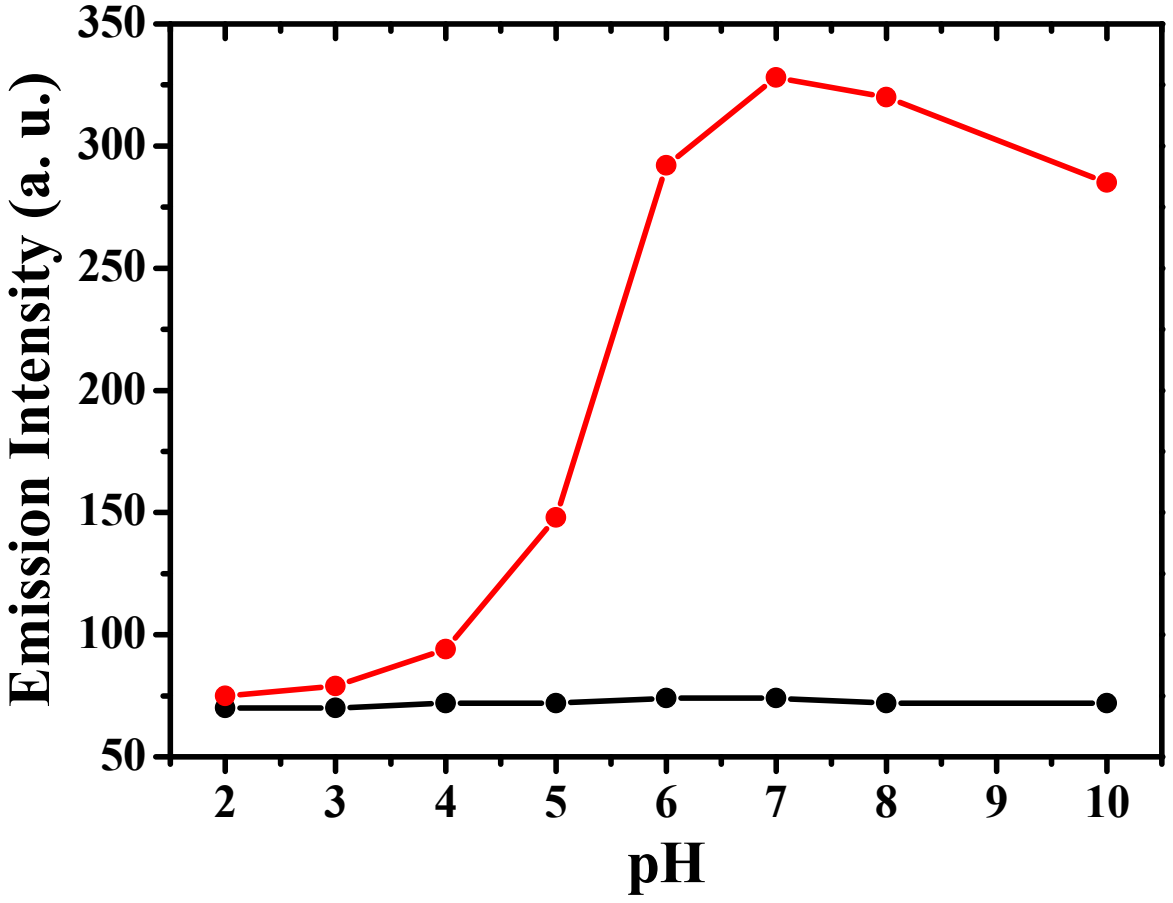

Fig. S14 Effect of pH on the emission intensity of **L** (5 μM) (black) and the [**L**–Al^{3+}] system (red) ([L] = [Al^{3+}] = 5 μM) (DMSO–H_2O (4:1, v/v), 0.1 M HEPES buffer, λ_{ex} = 330 nm, λ_{em} = 445 nm).

Table S1 Selected bond lengths (Å) and bond angles (°) for **L**

Bond lengths					
N(1)–C(21)	1.403(4)	C(3)–C(17)	1.425(5)	C(10)–C(16)	1.432(5)
N(2)–C(22)	1.342(4)	C(3)–C(4)	1.435(5)	C(11)–C(12)	1.346(6)
N(23)–C(24)	1.333(4)	C(4)–C(5)	1.348(5)	C(12)–C(13)	1.431(5)
N(25)–C(26)	1.339(4)	C(5)–C(6)	1.426(5)	C(13)–C(14)	1.386(5)
C(1)–N(1)	1.276(4)	C(6)–C(7)	1.394(6)	C(13)–C(17)	1.426(5)
C(22)–N(23)	1.353(4)	C(6)–C(16)	1.416(5)	C(14)–C(15)	1.388(5)
C(24)–N(25)	1.339(4)	C(7)–C(8)	1.386(6)	C(16)–C(17)	1.411(5)
C(1)–C(2)	1.478(5)	C(8)–C(9)	1.391(6)	C(21)–C(26)	1.377(5)
C(2)–C(15)	1.398(5)	C(9)–C(10)	1.399(6)	C(21)–C(22)	1.423(4)
C(2)–C(3)	1.417(5)	C(10)–C(11)	1.425(6)		
Bond angles					
N(1)–C(1)–C(2)	120.9(3)	C(3)–C(17)–C(13)	119.9(4)	C(14)–C(13)–C(12)	121.5(4)
N(1)–C(21)–C(22)	118.3(3)	C(4)–C(5)–C(6)	122.2(4)	C(14)–C(13)–C(17)	119.8(3)
N(2)–C(22)–C(21)	121.2(3)	C(5)–C(4)–C(3)	121.6(3)	C(14)–C(15)–C(2)	121.6(4)
N(23)–C(22)–C(21)	120.4(3)	C(6)–C(16)–C(10)	119.2(4)	C(15)–C(2)–C(1)	118.1(3)
N(25)–C(26)–C(21)	124.3(3)	C(7)–C(6)–C(5)	122.6(4)	C(15)–C(2)–C(3)	119.5(3)
N(2)–C(22)–N(23)	118.4(3)	C(7)–C(6)–C(16)	119.9(4)	C(15)–C(14)–C(13)	120.3(4)
N(23)–C(24)–N(25)	128.9(3)	C(7)–C(8)–C(9)	120.2(4)	C(16)–C(6)–C(5)	117.5(4)
C(1)–N(1)–C(21)	117.8(3)	C(8)–C(7)–C(6)	120.8(4)	C(16)–C(17)–C(3)	120.5(3)
C(24)–N(23)–C(22)	116.0(3)	C(8)–C(9)–C(10)	121.1(4)	C(16)–C(17)–C(13)	119.7(3)
C(26)–C(21)–N(1)	125.1(3)	C(9)–C(10)–C(11)	122.2(4)	C(17)–C(3)–C(4)	117.4(3)
C(24)–N(25)–C(26)	113.8(3)	C(9)–C(10)–C(16)	118.8(4)	C(17)–C(13)–C(12)	118.7(4)
C(2)–C(3)–C(4)	123.7(3)	C(11)–C(10)–C(16)	118.9(4)	C(17)–C(16)–C(6)	120.8(3)
C(2)–C(3)–C(17)	118.9(3)	C(11)–C(12)–C(13)	121.8(4)	C(17)–C(16)–C(10)	120.0(4)
C(3)–C(2)–C(1)	122.3(3)	C(12)–C(11)–C(10)	121.0(4)	C(26)–C(21)–C(22)	116.4(3)

Table S2 Selected hydrogen bond lengths (Å) and angles (°) for **L**

D–H···A	*d*(D–H)	*d*(H···A)	*d*(D···A)	∠(DHA)
N(2)–H(2A)···N(25)#1	0.870(10)	2.41(3)	3.137(4)	141(3)
N(2)–H(2B)···N(23)#2	0.881(10)	2.248(12)	3.123(4)	172(3)

Symmetry transformations used to generate equivalent atoms: #1 $x, y + 1, z$; #2 $-x, -y + 1, -z + 2$